Modelling of mobile robot with on board redundant manipulator arm

R.V.Ram[a] , P.M.Pathak[b] , and S.J.Junco[c]

Abstract

Manipulators with mobile base are gaining momentum in the industry due to improved workspace and flexible adaptability to changes in the product designs. Although there has been research in this field for a considerable time, many issues are still to be resolved viz. obstacle avoidance, redundancy resolution for singularity avoidance, dynamic analysis of combined manipulator and a mobile robot, base disturbances and optimized motion planning for limited power sources. Meticulous motion planning is a very essential for a mobile robot, particularly when it is carrying an on board manipulator.

In this work a three wheeled mobile robot (Robotino) with an on board redundant manipulator (MRBM) or simply mobile manipulator (MM) of eight degrees of freedom is considered for the analysis. Kinematic model of MM is developed first afterwards the Bond graph model of the mobile robot combined with manipulator is developed. Dynamic analysis is performed using the system equations generated from the bond graph model and simulation results are presented for different cases.

Keywords: mobile manipulator (MM), bond graph modeling, dynamic analysis

1. Introduction

Robot manipulators have become an integral part of every automated manufacturing system. There has been a constant search for improvement of the capabilities of the industrial robots. Workspace is a very crucial specification for an industrial robot and improvement of workspace will make them more viable. Mobile manipulator (MM) refers to the mounting of manipulator over a mobile base, which will not only enhance the work space but also gives greater flexibility for manipulation. The locomotion of the MM can be either legged locomotion or wheeled locomotion. Wheeled locomotion of a mobile robot is suitable for plain terrain and control is the easiest task. Whereas legged locomotion is applicable for uneven terrain, but it is a challenging to control it.

There has been extensive literature dealing with mobile manipulators. Carlton and Bartholet [1] presented a report on the development of a mobile manipulator for the maintenance of nuclear plant. They discussed the various technical requirements for development of mobile manipulator. Modelling of the MM is too complicated task since the modeling becomes compounded due to addition of mobile base. Bayle and Fourquet [2] presented kinematic modeling of nonholonomic wheeled mobile robot with planar manipulator. They discussed the nonholonomic conditions of mobile robots for various types of wheels. Salazar-Silva et al. [3] came up with a novel method for kinematic modeling of the mobile manipulator considering it as stationary robot. They considered it as a stationary robot having simultaneous locomotion and manipulator motion.Yamamoto and Yun [4] came up with the algorithm to coordinate the manipulator motion and locomotion of the mobile robot. They developed the control algorithm considering nonholonomic constraints of the mobile base for the path planning when the end effector position is known a priori.

Seraji [5] proposed on-line approach for motion control of rover mounted manipulator. An integrated kinematic model for manipulator mounted over a nonholonomic wheeled base was developed. Cohodar and

[a] PhD Scholar, Department of Mechanical and Industrial Engineering, IIT Roorkee, Roorkee, India. Email:rvitalram@gmail.com

[b]Associate Professor, Department of Mechanical and Industrial Engineering, IIT Roorkee , Roorkee, India. Email:pushpfme@iitr.ernet.in

[c] Professor Facultad de Ciencias Exactus, ingenieria y Agrimensura, Universidad Nacional de Rosario. Email:srgjunco@gmail.com

Omerspahic [6] did a dynamic analysis of Omni-three directional mobile robot. In this work modeling and simulation is carried out using Bond Graph approach. Minami et al. [7], proposed a novel criterion, avoidance manipulability shape index (AMSI) for avoiding an obstacle of a manipulator mounted on a mobile robot for measuring the avoidance ability of the mobile manipulator. Yamamoto and Yun [8] investigated the effects of the dynamic interaction between the manipulator and the mobile platform of a mobile manipulator on the task performance. Carrkier et al. [9] proposed a path planning algorithm for optimizing the length of the trajectory of mobile base. The simulated annealing method has been used to obtain the optimal solution.

Although there is abundant available literature, there is no generic modeling for kinematics and dynamics mobile manipulator. So in this work we developed the bond graph model of the mobile manipulator. The mobile manipulator becomes redundant when the number of degrees of freedom of manipulator exceeds three since the mobile base has already three degrees of freedom. In the past available literature the degrees of freedom of manipulator didn't exceed more than five because resolving the redundancy makes the problem more complex. In this work we considered a redundant manipulator mounted over a mobile base. The manipulator is an open chain with eight degrees of freedom and the mobile base has three degrees of freedom on a plain terrain. We considered a holonomic mobile base with three wheels and all are actuated using DC motors.

The outline of the work in this paper is as follow: in the section 2 the mechanical design of the redundant manipulator and the mobile base is given. In the next section 3 the mathematical background for the propagation of angular velocity and linear velocity are presented. In section 4 the integrated bond graph modeling of mobile base and the manipulator is given. In section 5 the validation of the model and base disturbance due to the motion of the manipulator is presented.

2. Mechanical Design

The schematic diagram of the mobile manipulator is shown in the Fig.1. The mobile base (bottom portion of Fig. 1) is a circular platform and is driven by three independently actuated Omni wheels. The three wheels are placed near the circumference and are at an angle of 120° to each other. The mobile base has three degrees of freedom, it can have linear motion in X and Y directions and can spin about Z-axis. Therefore, it is not subjected to non-holonomic constraints. Incorporation of the Omni wheels enhances the maneuverability, yet control is not the problem since the speed of locomotion has been considerably smaller (0.2 to 1.0 m/s). The manipulator is mounted at the center of the platform. The manipulator has eight degrees of freedom to make it more redundant and all joints are revolute joints. The higher redundancy gives more flexibility in manipulation, but also imposes challenge of finding the optimal trajectory for the required manipulation.

3. Mathematical Analysis

The bond graph modeling of the mobile manipulator depends on the development of the mathematical relationships for the kinematics and dynamics. The mathematical relations are given separately for the mobile base and manipulator.

3.1 Mathematical analysis of mobile base

The kinematics of the mobile base of the MM is calculated using the Fig.2. All the three wheels of the mobile base are of same radius R and the linear velocities V_1, V_2 and V_3 are along the tangents to the each wheel respectively. The velocities of the center of gravity (CG) of the base in longitudinal and lateral direction are the average of the algebraic sum of the longitudinal and lateral velocities of all wheels.

The velocity of the CG of base in the lateral direction (x direction) is:

$$V_x = \frac{\left[-V_2 + (V_1 - V_3)\sin(\frac{\pi}{6})\right]}{3} \tag{1}$$

Where, $V_1 = R\dot{\theta}_1$, $V_2 = R\dot{\theta}_2$, $V_3 = R\dot{\theta}_3$, and $\dot{\theta}_1$, $\dot{\theta}_2$ and $\dot{\theta}_3$ are angular velocities of wheels 1, 2 and 3, respectively, hence

$$V_x = \frac{R}{3}\left[-\dot{\theta}_2 + (\dot{\theta}_1 - \dot{\theta}_3)\sin(\frac{\pi}{6})\right] \quad (2)$$

The velocity of the CG in longitudinal direction (z direction) is

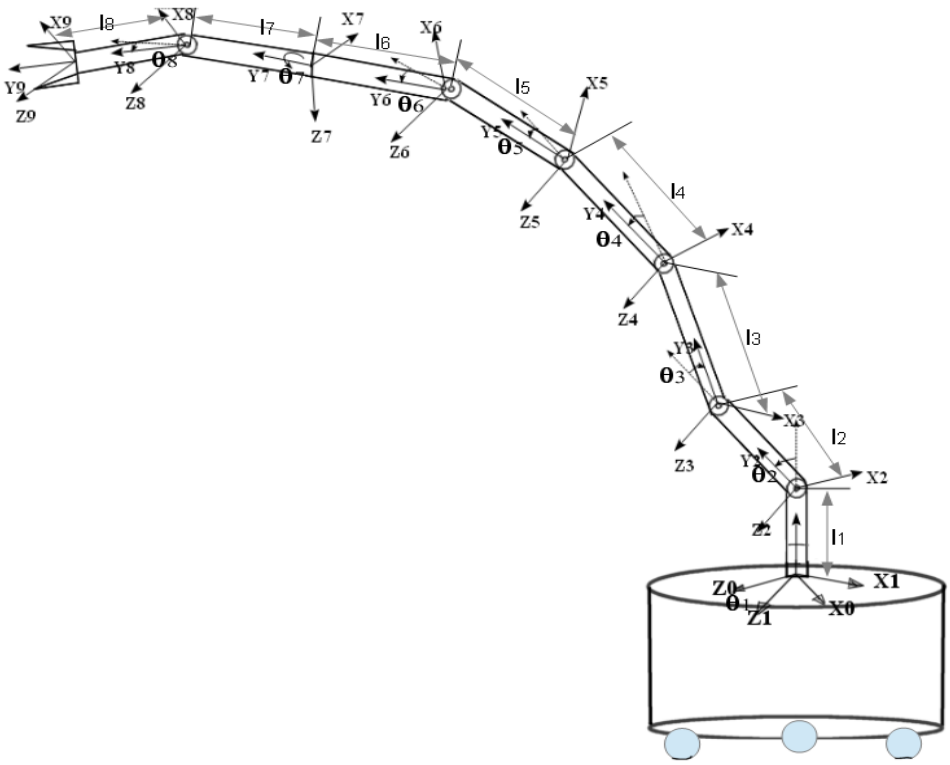

Figure 1: Schematic diagram of a mobile robot with manipulator

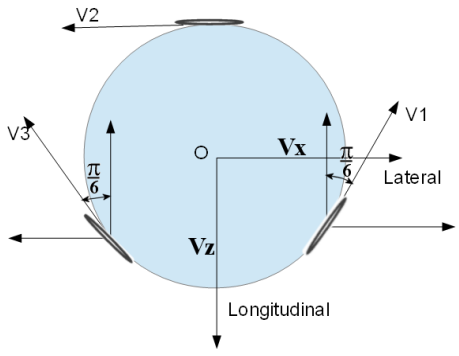

Figure 2: Velocities of mobile robot wheels

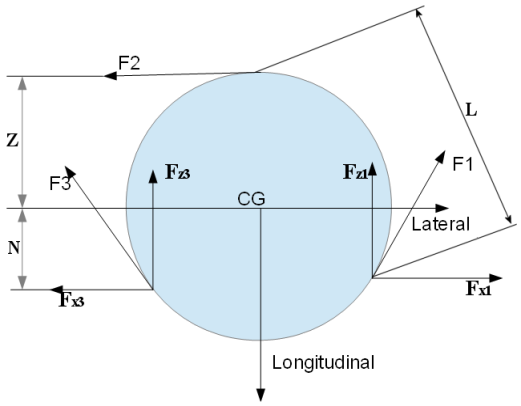

Figure 3: Forces in mobile robot wheels

$$V_z = (-\frac{R}{3})[\dot{\theta}_1 + \dot{\theta}_3]\cos(\frac{\pi}{6}) \tag{3}$$

The rotational velocity of the CG about the vertical axis is given by

$$\dot{\gamma} = \dot{\gamma}_1 + \dot{\gamma}_2 \tag{4}$$

Where, $\dot{\gamma}_1$ and $\dot{\gamma}_2$ are the rotational velocities produced due to relative velocities in z and x direction, as shown in Fig. 4.

$$\dot{\gamma}_1 = \frac{[V_1 - V_3]}{L}\cos(\frac{\pi}{6}) \qquad \text{and} \qquad \dot{\gamma}_2 = \frac{[V_2 + (V_1 - V_3)\sin(\frac{\pi}{6})]}{L} \tag{5}$$

Therefore, $$\dot{\gamma} = \frac{R}{L}[(\dot{\theta}_1 - \dot{\theta}_3)\cos(\frac{\pi}{6}) + \dot{\theta}_2 + (\dot{\theta}_1 - \dot{\theta}_3)\sin(\frac{\pi}{6})] \tag{6}$$

The dynamics of the mobile base are represented using the following equations and they are calculated based on the force vectors given in Fig. 3. F_1, F_2, and F_3 are the forces acting on the wheels and M is the mass of the mobile platform. The equations of motion for the rigid body are written using Euler's law as follows.

Equation of motion in the x direction is

$$M\dot{V}_x = -F_2 + (F_1 - F_3)\sin(\frac{\pi}{6}) + f_n V_x \tag{7}$$

Similarly, in z direction

$$M\dot{V}_z = -(F_1 + F_3)\cos(\frac{\pi}{6}) + f_m V_z \tag{8}$$

Where f_n and f_m are coefficients of friction in x and z directions

Equation of motion in rotation is obtained by taking moments about CG of the base. Hence, we get

$$I_z \ddot{\gamma} = (F_1 - F_3)\frac{L}{2}\cos(\frac{\pi}{6}) + (F_1 - F_3)N\sin(\frac{\pi}{6}) + F_2.z \tag{9}$$

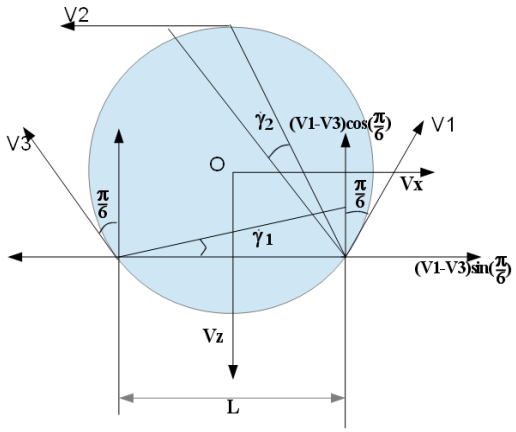

Figure 4: Relative velocity in x and z direction

3.2 Mathematical analysis of manipulator

The manipulator of the MM is as shown in the Fig. 1 has eight degrees of freedom. Using the transformation matrices the velocities are transformed from one link to another. The link 1 is placed on the mobile platform and it can rotate about a vertical axis and the other links are connected to each other to form an open chain. Coordinate frames are assigned to the base and the links as shown in the Fig. 1. The axis X_0, Y_0 and Z_0 are

assigned to the mobile base such that Y_0 axis is vertical. The coordinate frame X_1, Y_1 and Z_1 is assigned to link-1 and θ_1 is the angle of rotation of link 1 with respect to the base frame about the Y axis.

In this way coordinate frames are assigned to all the eight links. The link 1 and link 2 make an angle θ_2 with each other about z axis. The other links, link 3, 4, 5, 6 and 8 make an inclination of θ_3, θ_4, θ_5, θ_6, and θ_8 respectively, with previous link about Z axis but the link 7 makes an angle θ_7 with link 6 about Y axis. The end effector is attached to the end of link 8 and the frame X_9, Y_9 and Z_9 are appended to it. All the links are straight and the lengths of the links are l_1, l_2,…. l_8 respectively, of links 1, 2,…. 8.

The angular velocity propagation of the link from a link *i* to *i*+1 with reference to a frame *A* is given by [11]

$$ {}^{i+1}\left({}^{A}_{i+1}\omega\right) = {}^{i+1}_{i}R\left({}^{A}_{i}\omega\right) + {}^{i+1}\left({}^{i}_{i+1}\omega\right) \tag{10} $$

where ω is the angular velocity of the link and *R* is rotation transformation from *i* to *i*+1.

The linear velocity propagation of the link from link *i* to *i*+1 with reference to frame *A* is given by

$$ {}^{A}({}^{A}_{i+1}V) = [{}^{A}({}^{A}_{i}V)] + [{}^{A}_{i}R][-{}^{i}({}^{i}_{i+1}p\times)][{}^{i}({}^{A}_{i}\omega)] \tag{11} $$

where V represents the linear velocity of link and P represents the position vector of the link *i*+1 with reference to link *i*. The position vector P can be expressed in matrix form in terms of link length l_i as given below.

$$ [{}^{i}({}^{i}_{i+1}p)] = \begin{bmatrix} 0 & 0 & l_i \\ 0 & 0 & 0 \\ -l_i & 0 & 0 \end{bmatrix} \tag{12} $$

Using the above equation the angular and linear velocities of the link are calculated. All the different transformation matrices used are given in the appendix. Hence the bond graph model is developed based on these equations. The base of the manipulator is placed at the center of the mobile platform. Therefore the linear velocities and angular velocity of the mobile platform are transferred to the manipulator.

The manipulator linear velocity in x direction at base

$$ V_{x0} = V_x \tag{13} $$

The manipulator linear velocity in z direction at base

$$ V_{z0} = V_z \tag{14} $$

The manipulator linear velocity in y direction at base

$$ V_{y0} = 0 \tag{15} $$

The angular velocity of the manipulator in x and z directions

$$ \omega_{x0} = \omega_{Z0} = 0 \tag{16} $$

The angular velocity of the manipulator in y direction

$$ \omega_{y0} = \dot{\gamma} \tag{17} $$

4. Bond graph modeling of mobile manipulators

Bond graph is a modeling technique for modeling of dynamical systems, particularly applicable for systems with multi energy [10] domains such as electrical, mechanical, thermal, chemical, etc. Different elements in the bond graph are connected by half arrowed lines called bonds which represent the flow of the power in certain direction. Each bond carries power in the form of product flow and effort. Submodels are used in the bond graph to model the subsystems.

4.1 Bond graph modeling of mobile base

The bond graph of the mobile base is modeled using mathematical equations given the section 3.1. The three wheels of the mobile base are actuated using three individual motors and they are modeled using the Gyrator elements in bond graph as shown in Fig.5. The equations (2), (3) and (6) are used for kinematic modeling of the

mobile base and these equations give a linear velocity in x and z direction and angular velocity about y axis. Equations (7), (8) and (9) represents the dynamic equations which are also represented using bondgraph. The bond graph model of the mobile base takes input as the three input voltages for the motor and three force acting on the wheels and gives the velocities as output. The linear velocity in y direction and angular velocities in x and z direction are considered zero assuming it is moving on plane terrain. In the Fig.6 the bond graph model of mobile base is shown as submodel VRMB, which gives an output of three linear velocities and three angular velocities.

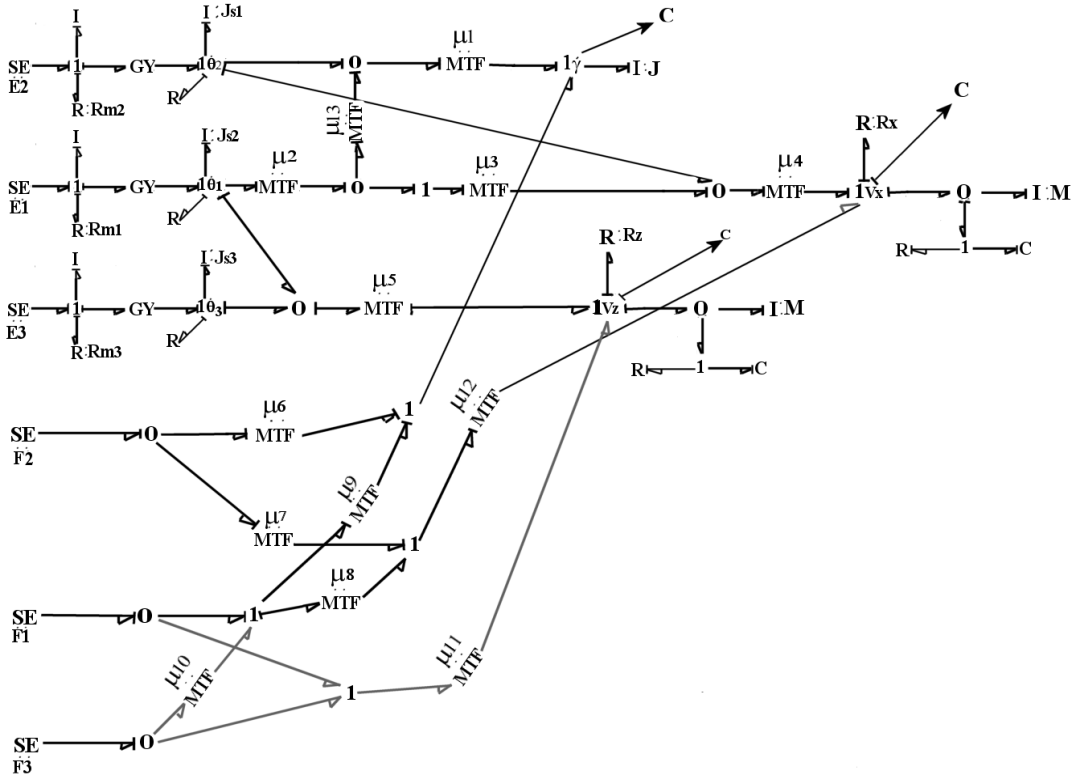

Figure 5: Bond graph modeling of the mobile base

4.2 Bond graph modeling of the manipulator

The manipulator has eight joints and each joint is actuated by a DC motor. In the bond graph model the joints are actuated by external torques represented by SE elements shown in the Fig. 6 without modeling of motor. The joint resistance is modeled using the R element. Each 1 junction in the model shown represent the angular velocity of each joint. The submodel AVD of link represent the propagation of the angular velocity of a link with respect to base from one link to next link following the equation (10). In this submodel the angular velocity with respect to the base of the present link is calculated as the sum of present link joint angular velocity and angular velocity of the previous link.

The submodel LVD of Link represents the propagation of the linear velocity vector of one link to the next. Following the equation (11) this submodel calculates the linear velocity of the present link using angular velocity of the present link, rotational transformation matrix with respect to previous link and linear velocity of the previous link. The submodel EJS represent the bond graph modelling of Euler Junction Structure (EJS). The EJS is the angular dynamic model of the rigid body. By adding the submodel of mobile base with the bond graph model of the manipulator, which is also made of various Submodels the combined bond graph model of the mobile manipulator is developed. The combined Bond graph model is developed in the SYMBOL SHAKTI software [13].

5. Simulation and validation of the model

The developed bond graph model of the mobile manipulator has been simulated for validation of the model. The Table 1 shows the parameter values chosen for the simulation purpose. The parameters of the simulation of the mobile base are given in the Table 2. The of the bond graph model of the mobile manipulator is validated by verifying the trajectory of the tip of the manipulator for the known joint angles.

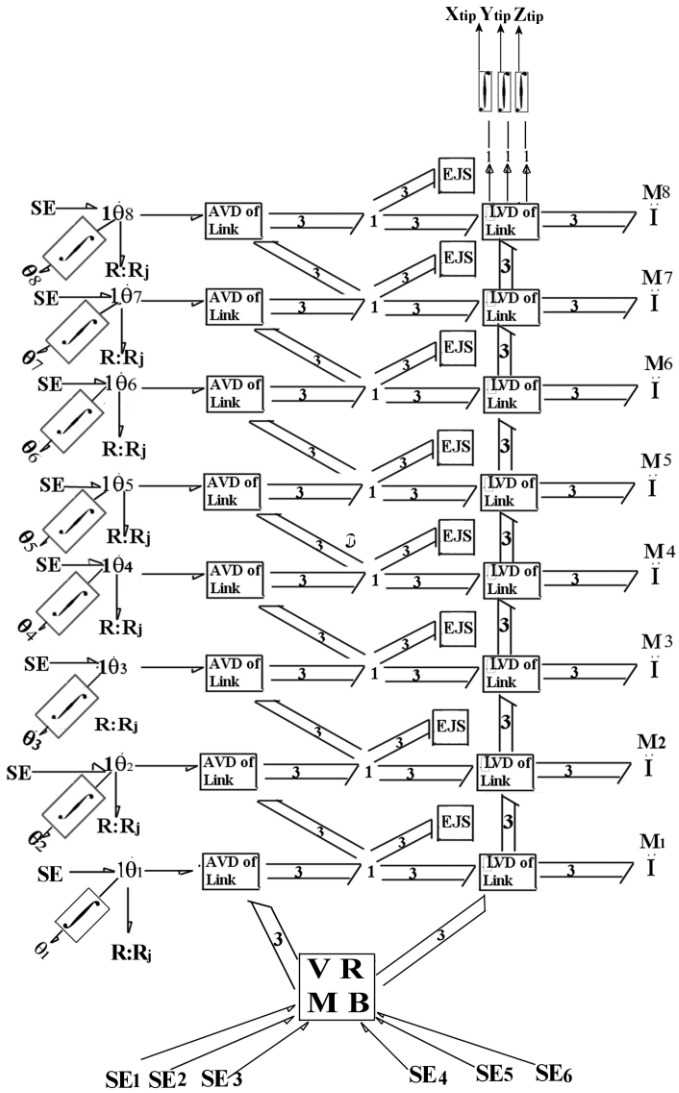

Figure 6: Bond graph model of mobile robot with manipulator

The manipulator is positioned such that all the joints are locked except the first joint and all the joint angles are zero except the second joint, which is kept at 90° (θ_2=1.571 radians). The schematic diagram of the orientation of the mobile manipulator for this case is shown in the Fig.6. When the first joint is actuated by giving a torque of 24 Nm to the joint, then the tip must make a circular trajectory of radius 1.6 m, which is sum of link lengths from link2 to link8 . From the bond graph model first order differential equations are derived, and in the simulator their numerical integration is done using a predictor - Corrector method. The simulation is performed for a time period of 5 seconds in the SYMBOLS Simulator module. The simulation results of the mobile manipulator when the mobile base is kept at rest condition by keeping all three wheels of the mobile base notactuated is shown in the Fig.7. It is clear from the figure that the tip is making a circular trajectory as the diameter is same in vertical and horizontal direction.

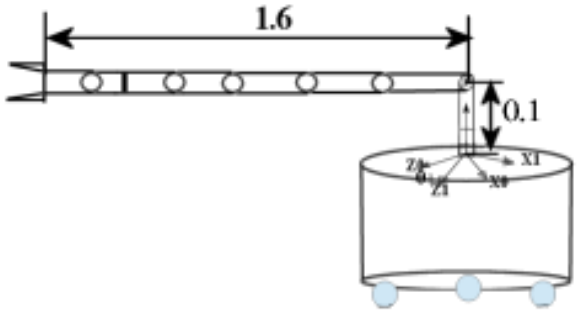

Figure 7: Initial configuration of mobile robot with manipulator

Table-1: Manipulator parameters

S.No	Link lengths (m)	Link masses (kg)	Mass moment of inertia (m^4)		
			I_{xx}	I_{yy}	I_{zz}
1	L_1=0.1	M_1=0. 5	0.002445	0.002039	0.002445
2	L_2=0.4	M_2=0.25	0.004004	0.0002	0.004004
3	L_3=0.3	M_3=0.25	0.00211	0.0002	0.00211
4	L_4=0.3	M_4=0.2	0.00211	0.0002	0.00211
5	L_5=0.2	M_5=0.2	0.0032032	0.00016	0.003202
6	L_6=0.2	M_6=0.15	0.0024024	0.002039	0.0024024
7	L_7=0.1	M_7=0.1	0.0016016	0.0008	0.0016016
8	L_8=0.1	M_8=0.1	0.0016016	0.0008	0.0016016

Table-2: Mobile base parameters

S.No	Parameters	Value
1	Mass	11kg
2	Moment of Inertia about vertical axis	0.1925kg-m^2
3	Moment of inertia of motor shaft	0.00071m^4
4	Motor inductance	0.2
5	Motor resistance	0.5ohm
6	Wheel friction coefficient in x and z direction	0.45

5.1 Base disturbance

The mobile base of the mobile manipulator is supposed to be stationary when its wheels are not actuated, but due to reaction to the manipulator motion there is some movement of the base. From the numerical simulation the base disturbance values are obtained and are plotted as shown in theFig.9. The figure shows the disturbance of the base in the form of rotation about the vertical axis and linear motion in x and z directions. It is observed that the reaction movement of the mobile base is increasing with time. The linear movement of the center of mass in x and z direction is very small but the rotation of the center of mass is gradually increasing with time.

The trajectory of the manipulator and base disturbance, are plotted for the case of wheels of manipulator are actuated and considering the contact forces of wheels as zero. These plots are shown in the Fig.10 and Fig.11. It is observed from the Fig.10 that the tip is making circular trajectory while the base is moving. The center of the circular trajectory is moving; therefore we can see the overlapped circles.

6. Conclusion

The Bond graph model of the mobile manipulator has been developed using the SYMBOL SHAKTI software. The model has been successfully validated by verifying the trajectory of the tip of the manipulator for the expected trajectory. It is observed that the mobile base has some reaction rotation even when its wheels are not actuated but the manipulator is actuated. The reaction linear movement of the CG of mobile base is just a few millimeters; therefore the tip trajectory of the manipulator is not effected. Also it is evident that when the mobile base has linear motion the center of trajectory of the tip is moving, and hence there are various circles overlapping.

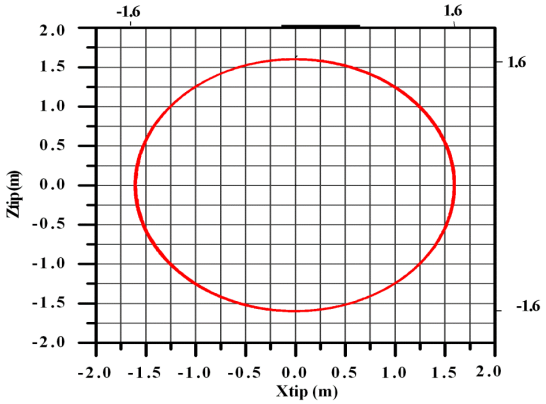

Figure 8: Manipulator tip trajectory without actuation of mobile base motors

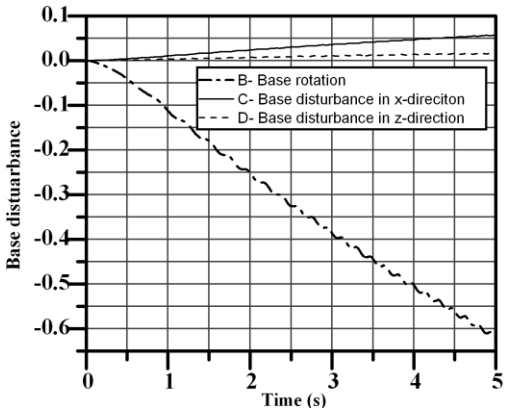

Figure 9: Disturbance of base without actuation of mobile base motor

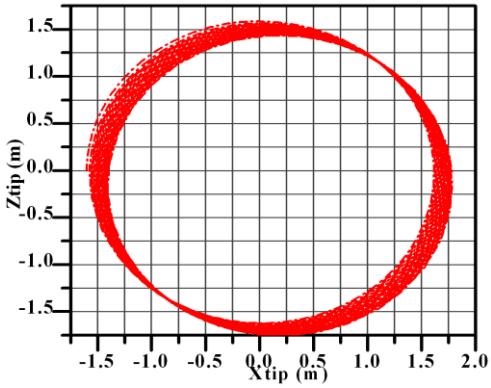

Figure 10: Manipulator tip trajectory with actuation of mobile base motors

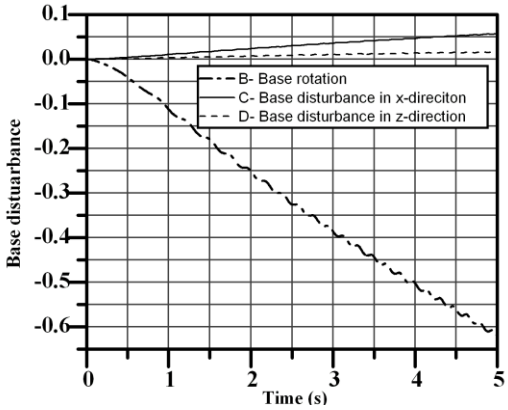

Figure11: Movement of base of the base with actuation of mobile base motors

References

1. R. E. Carlton and S. J. Bartholet, "The evolution of the application of mobile robotics to nuclear facility operations and maintenance" Proceedings of IEEE conference on Robotics and Automation, vol.2, pp. 720-726, 1987.

2. B. Bayle, and J-Y Fourquet, "Kinematic modeling of wheeled mobile manipulator", Proceedings of IEEE international conference on Robotics and Automation, 2003.

3. G.H. Salazar-Silva , Marco A. Moreno-Armendáriz, and Jaime Álvarez Gallegos " Modeling and Control in Task-Space of a Mobile Manipulator with Cancellation of Factory-Installed Proportional–Derivative Control", computacion y systems, vol. 16, No 4, 2012.

4. Y.Yamamoto and X.Yun, "Coordinating Locomotion and Manipulation of a Mobile manipulator", IEEE transactions on automatic control, vol. 39, no. 6, June 1994.

5. H. Seraji, "An on-line approach to coordinated mobility and manipulation", Proceedings of IEEE International Conference on Robotics and Automation, pp. 28-35, 1993.
6. M. Cohodar and A.Omerspahic, "Kinematic Modeling and Redundancy Resolution for nonholonomic Mobile Manipulators", Proceedings of the 2006 IEEE International Conference on Robotics and Automation - May 2006.
7 M. Minami, H. Tanaka, and Y.Mae, "Avoidance Ability of Redundant Mobile Manipulators During Hand Trajectory Tracking", Journal of Advanced Computational Intelligence and Intelligent Informatics, Vol.11 No.2, 2007.
8. Y. Yamamoto, and X.Yun, "Effect of the dynamic interaction on coordinated control of mobile manipulators", IEEE transactions on robotics and automation, vol. 12, no. 5, October 1996.
9. W. F. Carrikier, P. K. Khosla, and B. H. Krogh, "Path planning for mobile manipulators for multiple task execution", IEEE transactions on robotics and automation, vol. 7, no. 3, June 1991.
10. Merzouki, R., Samantaray, A. K., Pathak, P. M., and Bouamam, B. O. (2013). *Intelligent Mechatronic Systems: Modelling, Control and Diagnosis*. ISBN: 978-1-4471-4627-8 978-1-4471-4628-5, Springer, London.
11. J.J Craig, *Introduction to Robotics: Mechnanics and Control*, Pearson Education, 2004.
12 A. Mukharjee, R. Karmakar and A.K. Samantaray, *Bond Graph in Modeling, Simulation and Fault Identification*, I,K. Publications, 2006.
13. Users Manual of SYMBOLS Shakti, http://www.htcinfo.com/, *High-Tec Consultants, S.T.E.P.*, Indian Institute of Technology, Kharagpur, 2006.

Appendix

1. The transformation matrices used in the calculation of angular velocity propagation

$${}^{1}_{0}R=\begin{bmatrix} C_1 & 0 & -S_1 \\ 0 & 1 & 0 \\ S_1 & 0 & C_1 \end{bmatrix},\ {}^{2}_{1}R=\begin{bmatrix} C_2 & S_2 & 0 \\ -S_2 & C_2 & 0 \\ 0 & 0 & 1 \end{bmatrix},\ {}^{3}_{2}R=\begin{bmatrix} C_3 & S_3 & 0 \\ -S_3 & C_3 & 0 \\ 0 & 0 & 1 \end{bmatrix},$$

$${}^{4}_{3}R=\begin{bmatrix} C_4 & S_4 & 0 \\ -S_4 & C_4 & 0 \\ 0 & 0 & 1 \end{bmatrix},\ {}^{5}_{4}R=\begin{bmatrix} C_5 & S_5 & 0 \\ -S_5 & C_5 & 0 \\ 0 & 0 & 1 \end{bmatrix},\ {}^{6}_{5}R=\begin{bmatrix} C_6 & S_6 & 0 \\ -S_6 & C_6 & 0 \\ 0 & 0 & 1 \end{bmatrix},$$

$${}^{7}_{6}R=\begin{bmatrix} C_7 & 0 & -S_7 \\ 0 & 1 & 0 \\ S_7 & 0 & C_7 \end{bmatrix},\ \text{and}\ {}^{8}_{7}R=\begin{bmatrix} C_8 & S_8 & 0 \\ -S_8 & C_8 & 0 \\ 0 & 0 & 1 \end{bmatrix}$$

2. The transformation matrices used in the calculation of linear velocity propagation

$${}^{0}_{1}R=\begin{bmatrix} C_1 & 0 & S_1 \\ 0 & 1 & 0 \\ -S_1 & 0 & C_1 \end{bmatrix},\ {}^{0}_{2}R=\begin{bmatrix} C_1C_2 & -C_1S_2 & S_1 \\ S_2 & C_2 & 0 \\ -S_1C_2 & S_1S_2 & C_1 \end{bmatrix},\ {}^{0}_{3}R=\begin{bmatrix} C_1C_{23} & -C_1S_{23} & S_1 \\ S_{23} & C_{23} & 0 \\ -S_1C_{23} & S_1S_{23} & C_1 \end{bmatrix}$$

$$ {}^{0}_{4}R = \begin{bmatrix} C_1C_{234} & -C_1S_{234} & S_1 \\ S_{234} & C_{234} & 0 \\ -S_1C_{234} & S_1S_{234} & C_1 \end{bmatrix}, \qquad {}^{0}_{5}R = \begin{bmatrix} C_1C_{2345} & -C_1S_{2345} & S_1 \\ S_{2345} & C_{2345} & 0 \\ -S_1C_{2345} & S_1S_{2345} & C_1 \end{bmatrix}, $$

$$ {}^{0}_{6}R = \begin{bmatrix} C_1C_{23456} & -C_1S_{23456} & S_1 \\ S_{23456} & C_{23456} & 0 \\ -S_1C_{23456} & S_1S_{23456} & C_1 \end{bmatrix}, \quad {}^{0}_{7}R = \begin{bmatrix} C_1C_7C_{23456} - S_1S_7 & -C_1S_{23456} & C_1S_7C_{23456} + C_7S_1 \\ C_7S_{23456} & C_{23456} & S_7S_{23456} \\ -C_7S_1C_{23456} - C_1S_7 & S_1S_{23456} & -S_1S_7C_{23456} + C_1C_7 \end{bmatrix} $$

$$ {}^{0}_{8}R = \begin{bmatrix} [C_1C_7C_8C_{23456} - S_1S_7C_8] + C_1S_8S_{23456} & C_1C_7S_8C_{23456} - S_1S_7S_8 - C_1C_8S_{23456} & C_1S_7C_{23456} + C_7S_1 \\ C_7C_8S_{23456} - S_8C_{23456} & C_7S_8S_{23456} + C_8C_{23456} & S_7S_{23456} \\ -C_7C_8S_1C_{23456} - C_1C_8S_7 - S_1S_8S_{23456} & C_7S_1S_8C_{23456} - C_1S_7S_8 + S_1C_8S_{23456} & -S_1S_7C_{23456} + C_1C_7 \end{bmatrix} $$

Where $S_i = \sin\theta_i,\ for 1 \le i \le 8$ and $C_i = \cos\theta_i,\ for 1 \le i \le 8$

$S_{23} = \sin(\theta_2 + \theta_3)$ and $C_{23} = \cos(\theta_2 + \theta_3)$

$S_{234} = \sin(\theta_2 + \theta_3 + \theta_4)$, $C_{234} = \cos(\theta_2 + \theta_3 + \theta_4)$

$S_{2345} = \sin(\theta_2 + \theta_3 + \theta_4 + \theta_5)$ and $C_{2345} = \cos(\theta_2 + \theta_3 + \theta_4 + \theta_5)$

$S_{23456} = \sin(\theta_2 + \theta_3 + \theta_4 + \theta_5 + \theta_6)$ and $C_{23456} = \cos(\theta_2 + \theta_3 + \theta_4 + \theta_5 + \theta_6)$